

## Uniformly Colored Beads for Multiplex Immunoassay

Xiang-Wei Zhao,<sup>†,‡</sup> Zhao-Bin Liu,<sup>‡</sup> Han Yang,<sup>‡</sup> Keiji Nagai,<sup>§</sup> Yu-Hua Zhao,<sup>†</sup> and Zhong-Ze Gu<sup>\*‡</sup>

College of Life Science, Zhejiang University, Hangzhou 310029, China, State Key Laboratory of Bioelectronics, Southeast University, Nanjing 210096, China, and Institute of Laser Engineering, Osaka University, Osaka 565-0871, Japan

Received February 4, 2006. Revised Manuscript Received March 9, 2006

We introduced a fluidic droplet generation method for the generation of monodispersed polymer beads with structural color. Multicolored polystyrene beads were derived by embedding pearl pigment. Methods for generating uniform color and controlling bead size and surface were developed to make the beads suitable for multiplex immunoassay. A multiplex assay of antigen–antibody interaction shows that the multicolored encoded bead is a stable and cost-effective microcarrier. Wide applications in genomic or proteomic studies, drug screening, clinical diagnostics, and combinatorial chemical fields are anticipated.

### Introduction

High throughput and miniaturization are two important areas of research for biological and chemical analysis.<sup>1,2</sup> Genomics, proteomics, and combinatorial chemistry applications lead to the emergence of various encoding strategies on large numbers of molecules which can speed up and simplify the assays in a multiplexed format.<sup>3,4</sup> Most of the assays such as gene expression, drug discovery, and clinical diagnostics are based on molecular binding or recognition events. Hence, in order to distinguish different binding events in parallel, different molecules are conjugated to different supports or labels, which can mark the molecules clearly. In comparison with conventional biological or chemical analysis, different molecules could be analyzed simultaneously when biomolecules are encoded. Obviously, the advantage of the multiplexed assay is that the time, cost, and samples of the assay are saved.

The existing encoding strategies employ coordinate-addressed arrays or fluidic encoded carriers. The coordinate-encoding technique is most commonly used in DNA and protein array analysis in which the probe molecules are immobilized on a substrate and encoded by the coordinate of its position. Although the coordinate-addressed microarrays are well-commercialized as a powerful technical platform, the molecular binding kinetics on the substrate is diffusion-limited, which slows the analysis speed.<sup>5</sup> Recently, mobile supports (carriers) with fluorescent molecules, vibrational signatures, quantum dots, discrete metallic layers,

photonic crystals, shape, or radio frequency as encoded elements attract more and more attention.<sup>6–16</sup> These fluidic microparticles can be mixed and subjected to an assay simultaneously. Each microparticle acts as a “microlab” that detects a corresponding molecule in the complex mixture. The fluidic microparticles are more flexible in application, faster in binding kinetics, and less expensive in cost.<sup>17</sup>

Multiplex detection is often the method of choice for efficiently deciphering functions or structures of multiple analytes simultaneously in a biological sample.<sup>18</sup> The encoded microparticles can have applications in the multiplex immunoassay of disease (e.g., viral or bacterial infections, cancer, and thrombosis), environmental pollutants, and weapons of mass destruction (chemical and biological weapons) and so on. And multiplex immunoassays in which two or more analytes are measured simultaneously in a single

\* To whom correspondence should be addressed. Fax: 86-25-83795635. E-mail: gu@seu.edu.cn.

<sup>†</sup> Zhejiang University.

<sup>‡</sup> Southeast University.

<sup>§</sup> Osaka University.

- (1) Battersby, B.; Trau, M. *Trends Biotechnol.* **2002**, *20*, 167–173.
- (2) Verpoorte, E. *Lab Chip* **2003**, *3*, 60N–80N.
- (3) Braeckmans, K.; De Smedt, S.; Leblans, M.; Pauwels, R.; Demeester, J. *Nat. Rev. Drug. Discovery* **2002**, *1*, 447–456.
- (4) Cullen, C. J.; Wootton, R. C. R.; de Mello, A. J. *Curr. Opin. Drug. Discovery Dev.* **2004**, *7*, 798–806.
- (5) Ferguson, J.; Steemers, F.; Walt, D. *Anal. Chem.* **2000**, *72*, 5618–5624.

- (6) Fulton, R. J.; McDade, R. L.; Smith, P. L.; Kienker, L. J.; John R.; Kettman, J. *Clin. Chem.* **1997**, *43*, 1749–1756.
- (7) Fenniri, H.; Hedderich, H.; Haber, K.; Achkar, J.; Taylor, B.; Ben-Amotz, D. *Angew. Chem., Int. Ed.* **2000**, *39*, 4483–4485.
- (8) Han, M.; Gao, X.; Su, J.; Nie, S. *Nat. Biotechnol.* **2001**, *19*, 631–635.
- (9) Nicewarner-Pena, S. R.; Freeman, R. G.; Reiss, B. D.; He, L.; Pena, D. J.; Walton, I. D.; Cromer, R.; Keating, C. D.; Natan, M. J. *Science* **2001**, *294*, 137–141.
- (10) Cunin, F.; Schmedake, T.; Link, J.; Li, Y.; Koh, J.; Bhatia, S.; Sailor, M. *Nat. Mater.* **2002**, *1*, 39–41.
- (11) Pantano, P.; Meek, C.; Wang, J.; Coutinho, D.; Balkus, K. *Lab Chip* **2003**, *3*, 132–135.
- (12) Vaino, A. R.; Janda, K. D. *P. Natl. Acad. Sci. U.S.A.* **2000**, *97*, 7692–7696.
- (13) Xu, H. X.; Sha, M. Y.; Wong, E. Y.; Uphoff, J.; Xu, Y. H.; Treadway, J. A.; Truong, A.; O'Brien, E.; Asquith, S.; Stubbins, M.; Spurr, N. K.; Lai, E. H.; Mahoney, W. *Nucleic Acids Res.* **2003**, *31*, e43.
- (14) Chen, Z.; Tsai, J.; Merriman, B.; Chen, J.; Kim, C.; Nelson, S. *Am. J. Hum. Genet.* **2003**, *73*, 434–434.
- (15) Meiring, J. E.; Schmid, M. J.; Grayson, S. M.; Kirby, R.; Manthiram, K.; Hsia, B. I.; Ellington, A. D.; Willson, C. G. *Abstr. Pap. Am. Chem. Soc.* **2004**, *227*, U515–U515.
- (16) Moran, E. J.; Sarshar, S.; Cargill, J. F.; Shahbaz, M. M.; Lio, A.; Mjalli, A. M. M.; Armstrong, R. W. *J. Am. Chem. Soc.* **1995**, *117*, 10787–10788.
- (17) Fu, A. Y.; Spence, C.; Scherer, A.; Arnold, F. H.; Quake, S. R. *Nat. Biotechnol.* **1999**, *17*, 1109–1111.
- (18) Su, X.; Zhang, J.; Sun, L.; Koo, T.; Chan, S.; Sundararajan, N.; Yamakawa, M.; Berlin, A. *Nano Lett.* **2005**, *5*, 49–54.

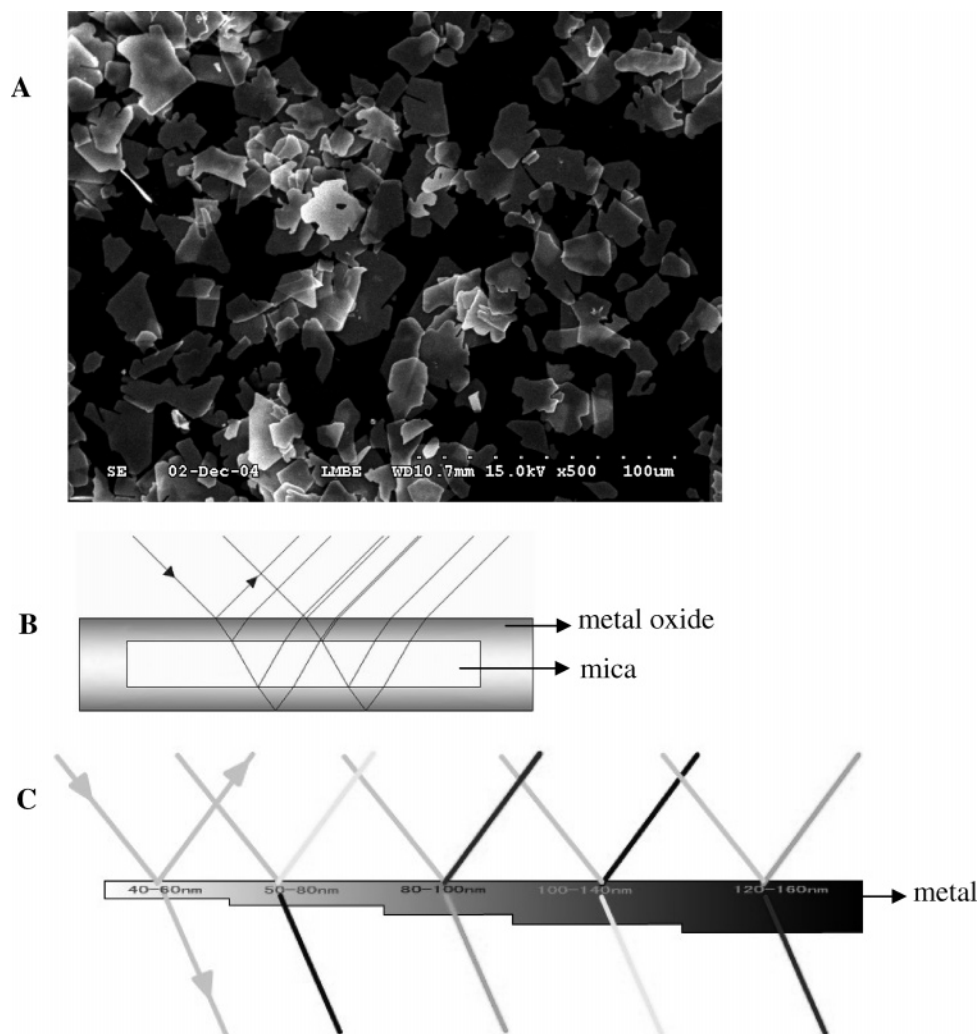


**Figure 1.** (A) SEM image of pearl pigment. (B and C) Illustrations showing the mechanics of pearl pigment color.

assay represent the next major advance in immunoassay methodology. It uses fewer samples in order to miniaturize the assay, increase the test throughput, and decrease the overall cost per test.<sup>19</sup>

The encoded microparticles are usually polymer spheres with diameter of 0.3  $\mu\text{m}$  to 6  $\mu\text{m}$ .<sup>6,20–25</sup> Usually, the small size spheres are used for high-throughput screening, while the large spheres are used for multiplex immunoassays.<sup>6–10,21,26</sup> And the desired encoding strategies are those which are cost-effective, are amenable to simplification, and automate the decoding process.<sup>27</sup> One of the candidates is the optically encoded microcarriers. Up to now the well-used encoding elements are generally fluorescence dyes, which are chemi-

cally unstable (such as photobleaching and photoquenching).<sup>28</sup> This problem can be partially improved by using semiconductor quantum dots.<sup>29,30</sup> Recently, Sailor et al. proposed the use of flat porous silicon particles, a kind of photonic crystal, as the encoded microcarriers.<sup>10,31</sup> The structural colorized microcarrier has the advantage in that the code is not only stable but also easy to be decoded under low optical resolution. In this paper, we would like to induce the fabrication and application of a new type of photonic crystal encoded microcarriers, which are polystyrene beads embedded with pearl pigment as the encoding element.

Pearl pigment is a kind of photonic crystal composed of a plate of mica with a layer of metal oxide film such as titania film on its surface (Figure 1). When the pigment is irradiated, light is reflected at the air/metal oxide and metal oxide/mica interfaces. The interference of the reflected light results in a definite color, which depends on the thickness of the metal oxide film. The color of the pearl pigment is easily designed by varying the thickness of the metal oxide layer. Due to the pearl pigment being made of stable materials, the color

(19) Gooding, C.; Choudary, P. *J. Microbiol. Methods* **1998**, *34*, 89–98.  
 (20) Park, M. K.; Briles, D. E.; Nahm, M. H. *Clin. Diagn. Lab. Immunol.* **2000**, *7*, 486–489.  
 (21) Harma, H.; Aronkyto, P.; Lovgren, T. *Anal. Chim. Acta* **2000**, *410*, 85–96.  
 (22) Zhi, Z.-I.; Morita, Y.; Hasan, A.; Tamiya, E. *Anal. Chem.* **2003**, *75*, 4125–4131.  
 (23) Hakala, H.; Virta, P.; Salo, H.; Ionnberg, H. *Nucleic Acids Res.* **1998**, *26*, 5581–5588.  
 (24) Michael, K. L.; Taylor, L. C.; Schultz, S. L.; Walt, D. R. *Anal. Chem.* **1998**, *70*, 1242–1248.  
 (25) Swartzman, E. E.; Miraglia, S. J.; Mellentin-Michelotti, J.; Evangelista, L.; Yuan, P. M. *Anal. Biochem.* **1999**, *271*, 143–151.  
 (26) Battersby, B. J.; Lawrie, G. A.; Trau, M. *Drug Discovery Today* **2001**, *6*, S19–S26.  
 (27) Czarnik, A. W. *Curr. Opin. Chem. Biol.* **1997**, *1*, 60–66.

(28) Bencic-Nagale, S.; Walt, D. R. *Anal. Chem.* **2005**, *77*, 6155–6162.  
 (29) Bruchez, M., Jr.; Moronne, M.; Gin, P.; Weiss, S.; Alivisatos, A. P. *Science* **1998**, *281*, 2013–2016.  
 (30) Chan, W. C. W.; Nie, S. *Science* **1998**, *282*, 2016–2018.  
 (31) Meade, S. O.; Yoon, M. S.; Ahn, K. H.; Sailor, M. J. *Adv. Mater.* **2004**, *16*, 1811–1814.

is able to bear acid or alkali, withstand temperatures as high as 800 °C, be stable to light irradiation, and be innocuous to humans. Therefore, unlike other encoding methods employing organic or fluorescent dye as the encoding element,<sup>32,33</sup> problems such as photobleaching, photoquenching, photostability, or chemical instability do not exist with the pearl pigment. In addition, the structural color of the code elements could be identified even by the naked eye if the reflection falls into the visible region. With a droplet generator we prepared multicolored beads encoded with pearl pigment. A multiplex bioassay based on antigen–antibody interactions demonstrates that the multicolored beads could be used as a kind of encoding support for biological applications.

### Methods

**Materials.** Polystyrene (PS, molecular weight: 158000) was from Yangtze Petrochemical Co., Ltd. Poly(vinyl alcohol) (PVA) (polymerization degree: 500) was obtained from VAM & POVAL Co., Ltd, Japan. Benzene and 1,2-dichloroethane were bought from Shiyi Chemical Reagent Co., Ltd., and Jiuyi Chemical Reagent Co., Ltd., respectively. Pearl pigments were gifts from Dongzhu Pearlescent Pigments Manufacturing Co., Ltd. Trimethylchlorosilane was from Sinopharm Chemical Reagent Co., Ltd. Human IgG, rabbit IgG, mouse IgG, and three kinds of FITC (fluorescein isothiocyanate) tagged goat anti-human IgG, goat anti-mouse IgG, and FITC tagged goat anti-rabbit IgG were obtained from Biodee Biotechnology Co., Ltd., Beijing. Phosphate buffer saline (PBS, 0.05 M, pH7.4), Phosphate buffer saline tween-20 (PBST, 0.05% tween-20 in PBS) and sodium carbonate buffer (SCB, 0.05 M, pH9.6) were self-prepared. Double-distilled water was used for all the experiments.

**Equipment.** A droplet generator apparatus (Figure 2) was used to prepare the pearl pigment contained polystyrene beads.<sup>34</sup> The apparatus is composed of three main parts: the flux controller, the droplet generator, and the collector. The flux controller includes an automatic syringe pump, and a magnetic pump equipped with a flowmeter. The syringe pump is used to control the flowing velocity of the oil-phase PS solution, while the magnetic pump and the flowmeter are used to control the flow velocity of water-phase PVA solution. The droplet generator is a cylinder made of organic glass. A glass tube with orifice 3 at the end drills through the center of the cylinder's coping. The oil-phase solution is fed by the injector through orifice 1 to the center glass tube and water-phase solution is fed through orifice 2 to the cylinder. The drops of oil-phase solution form out of orifice 3 and are taken into the collector (beaker or flask) by the flux of the water-phase solution.

Digital images of color beads were derived by scanning using an EPSON PERFECTION 1670 scanner. Scanning electron microscope (SEM) observations were performed using a HITACHI S-3000N Scanning Electron Microscope. X-ray photoelectron spectra (XPS) analysis was carried out on an ESCALB MK II spectrometer using Mg K $\alpha$  radiation. Protein solution fluorescence was measured by a Perkin-Elmer LS 55 luminescence spectrometer. Bright field and fluorescence microscope images were captured with a Leica TCS SP II confocal laser scan microscope (CLSM).

**Bead Preparation.** The photo-encoded beads were prepared with the droplet generator shown in Figure 2. Polystyrene was dissolved

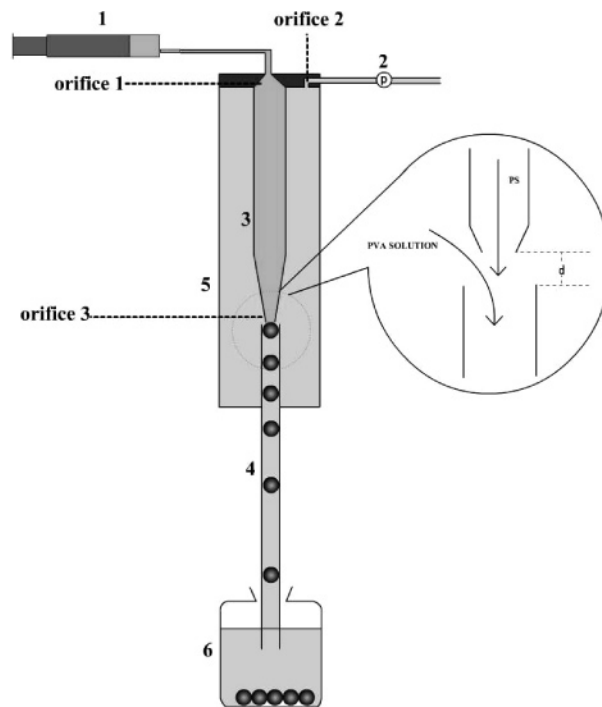


**Figure 2.** Sketch of the droplet generator. PS: polystyrene; PVA: Poly(vinyl alcohol); 1: syringe pump; 2: magnetic pump; 3: glass tube; 4: glass tube; 5: cylinder; 6: collector.

in a mixture of 2:3 benzene and 1,2-dichloroethane to the concentration of 7%. The density of the solution was adjusted to 1.045 g/cm<sup>3</sup> with the two organic solvents. And the solution was filtrated through a 0.2  $\mu$ m core filter before use. Pearl pigments were mixed with 10% trimethylchlorosilane in toluene and then filtered and baked at 80 °C for 2 h before they were dispensed in the polystyrene solution overnight with continuous agitation. The polystyrene solution was continuously fed through orifice 1 to the glass cylinder in which there is a stable flow of water solution containing 5% PVA. Feeding the polymer solution through the orifice results in droplets in the PVA water solution and the droplets were collected in a beaker. Rotary evaporation was employed to evaporate the benzene and 1,2-dichloroethane in the droplets in order to solidify the droplets. The evaporation temperature was from room temperature to 70 °C by increments of 5 °C per 10 min. And the rotary speed was set to 40 rpm. Finally, to remove the PVA on the bead surface, the solidified beads were ultrasonically washed eight times, each time for 15 min at 80 °C before the following assays. XPS analysis of the titanium element was performed on the pearl pigment and beads surface, respectively.

**Protein Adsorption and Multiplex Bioassay.** For protein adsorption capacity measurement, 100 ultrasonic-washed beads with diameter of 0.5 mm were coated with 100  $\mu$ L of human FITC tagged goat anti-human IgG (5  $\mu$ g/mL) at 4 °C overnight after 1 h of incubation at room temperature. The beads were washed with PBS buffer (pH 7.4) three times each for 5 min. The protein solution after coating and the washing filtrate were collected, and the solutions were measured with a LS 55 luminescence spectrometer and the protein concentration was calculated according to the fluorescence standard curve of FITC tagged goat anti-human IgG. The adsorbed protein was the protein in the coating solution minus that of the coating solution and diluted solution. The capacity was calculated by dividing the adsorbed protein with the surface area of the beads.

Red, yellow, and green polystyrene beads (~400  $\mu$ m), 100  $\mu$ L, were coated with human IgG (10  $\mu$ g/mL), rabbit IgG (10  $\mu$ g/mL), and mouse IgG (10  $\mu$ g/mL) in SCB buffer (pH 9.6), respectively.

(32) Kettman, J.; Davies, T.; Chandler, D.; Oliver, K.; Fulton, R. *Cytometry* **1998**, *33*, 234–243.

(33) Lawrie, G. A.; Battersby, B. J.; Trau, M. *Adv. Funct. Mater.* **2003**, *13*, 887–896.

(34) Nagai, K.; Nakajima, M.; Norimatsu, T.; Izawa, Y.; Yamanaka, T. *J. Polymer. Sci., A: Polym. Chem.* **2000**, *38*, 3412–3418.



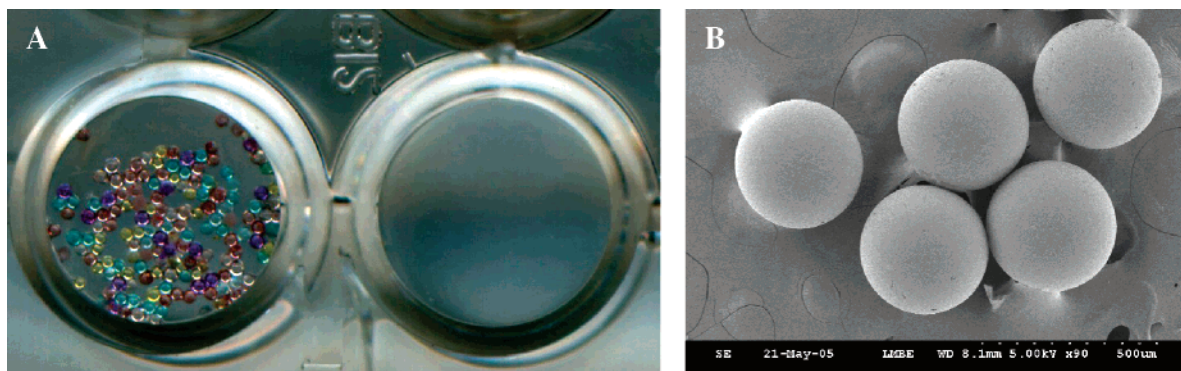


**Figure 3.** (A) Multicolored beads in a well of a 96-well microplate; (B) SEM image of beads of uniform color.

After being washed with PBS three times, the beads were blocked with bovine serum albumin (BSA, 1% in PBS) for 2 h at room temperature. And then three kinds of color beads were mixed together and incubated with continuous shaking for 1 h in the presence of solution containing FITC tagged goat anti-human IgG and goat anti-rabbit IgG (1:100 titer) at 37 °C. Last, the beads were washed with PBST and PBS three times for 5 min successively. The fluorescence images were captured under a CLSM with exciting wavelength at 488 nm and emission wavelength at 500–530 nm. To decode the color of the beads, bright field images were taken.

### Results and Discussion

The principle of the generator is that oil-phase polystyrene solution turns into droplets when it is injected into the flux of water-phase poly(vinyl alcohol) solution through a glass orifice as shown in Figure 2. After the organic solvent in the droplets is evaporated up in a rotary evaporator, the droplets turn into polystyrene beads. Using the droplet generator apparatus we prepared encoded polystyrene beads of different colors and homogeneous surfaces (Figure 3).

Figure 1A is the SEM image of red pearl pigment powder. The powder consists of flakes with sizes from 10 to 60  $\mu\text{m}$ . If the flakes are directly used as supports for biological or chemical assays, the following problems should be considered. First, the optical decoding system should be of high resolution due to the small sizes of the flakes. Second, it is difficult to sort the flakes due to their irregular shapes. Third, coagulation of the flakes during the detection process will prohibit the interaction of the target molecules in the solution with the probe molecules on the flake surface. Fourth, spatial orientation of the flakes should be controlled during the decoding process. Furthermore, the flakes are fragile. These problems can be solved by embedding the pearl pigment into polymer spheres and using polymer spheres as carriers of probe molecules.<sup>8,35–37</sup> Here, polystyrene, which is commonly employed in the fabrication of an immunoassay microtiter plate, is used to embed the pearly pigment because it can strongly absorb protein molecules by the force of hydrophobic interaction and exhibits excellent mechanical, chemical, and optical properties.<sup>38</sup>

In the droplet generator, when the polystyrene solution was squeezed out of orifice 3, it turned into spherical droplets in the flux of PVA solution because the surface tension preferred to reduce its surface area to decrease the surface energy. Here, the surfactant PVA existing at the water/oil interface could increase the stability of the oil-phase droplets and the viscosity of the water-phase solution, which prevented the droplets from collapse, agglomeration, and adherence to the wall of the container. To obtain spherical beads, it is very important to match the densities of the oil-phase solution and the water-phase PVA solution. The reason is that if the density of the oil solution is much higher than that of the water solution, the oil droplets will sink to the bottom of the container and deform due to gravity. In contrast, if the density of the oil solution is much lower than that of the water solution, the drops will float on the water and collapse. Only when the density of the oil solution is matched to the water solution can the oil droplets stably suspend in the solution.<sup>39</sup> In our experiment, we used benzene (0.88 g/cm<sup>3</sup>) and 1,2-dichloroethane (1.26 g/cm<sup>3</sup>) to adjust the density of the oil solution. Because boiling points of the solvents (benzene  $\sim$ 353 K; 1,2-dichloroethane  $\sim$ 356 K) are close, the density of droplets will not change much during the whole evaporation process. The size of the droplets depends on four parameters: the caliber of the orifice ( $c$ ), the velocity of the polystyrene ( $v_{\text{PS}}$ ), the velocity of PVA ( $v_{\text{PVA}}$ ), and the distance between orifice 3 and the glass tube ( $d$ ). In general, the size of the droplets increases when  $v_{\text{PS}}$  increases,  $v_{\text{PVA}}$  decreases, or  $d$  increases. The size of the encoded polystyrene beads also increases when the concentration of polystyrene in solution increases. Up to now, beads with diameter of 0.1–3 mm are fabricated by the control of these parameters. Figure 4 shows some beads of different sizes. For these parameters, we found that the control of velocity of polystyrene can result in beads of different sizes with better repeatability. The first reason is that the velocity of PVA solution (mL/min) is much higher than that of PS solution ( $\mu\text{L}/\text{min}$ ) and a little variance in the  $v_{\text{PVA}}$  will cause a big variance in the bead size. The second reason is that the  $v_{\text{PS}}$  is more precisely controlled than the distance between orifice 3 and the glass tube. Figure 5 shows the dependence of the bead sizes on  $v_{\text{PS}}$ . In this figure the polystyrene

(35) Yamada, Y.; Sakamoto, T.; Gu, S.; Konno, M. *J. Colloid Interface Sci.* **2005**, *281*, 249–252.

(36) Braeckmans, K.; De Smedt, S.; Roelant, C.; Leblans, M.; Pauwels, R.; Demester, J. *Nat. Mater.* **2003**, *2*, 169–173.

(37) Moreira, R.; Havranek, M.; Sames, D. *J. Am. Chem. Soc.* **2001**, *123*, 3927–3931.

(38) Kusnezow, W.; D. Hoheisel, J. *J. Mol. Recognit.* **2003**, *16*, 165–176.

(39) Nagai, K.; Norimatsu, T.; Izawa, Y.; Yamanaka, T. *Encyclopedia of Nanoscience and Nanotechnology*; American Scientific Publishers: Stevenson Ranch, CA, 2004; 10, 407–420.

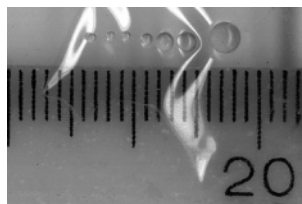


**Figure 4.** Beads of different sizes. The sizes of the beads from left to right were 0.48, 0.53, 0.62, 0.63, 0.95, 1, and 1.7 mm when the velocity of polystyrene solution was 105, 115, 135, 140, 210, 220, and 370  $\mu\text{L}/\text{min}$ , respectively, and  $c = 200 \mu\text{m}$ ,  $v_{\text{PVA}} = 25 \text{ mL}/\text{min}$ , and  $d = 0.5 \text{ mm}$ . The scale of the ruler is  $2/3 \text{ mm}$ .

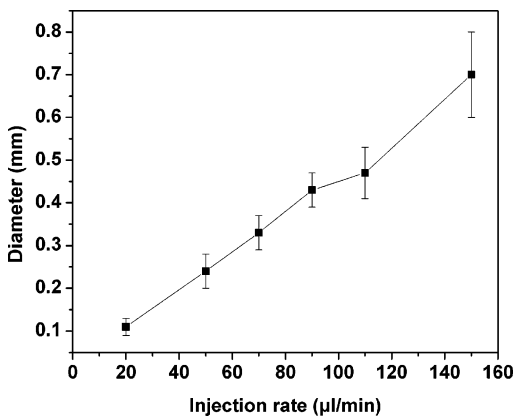


**Figure 5.** Relationship between bead diameter and injection rate of PS solution.

concentration is 7%,  $c = 200 \mu\text{m}$ ,  $v_{\text{PVA}} = 25 \text{ mL}/\text{min}$ , and  $d = 0.5 \text{ mm}$ . The diameter of the bead was  $110 \mu\text{m}$  when the injection speed of polystyrene was  $20 \mu\text{L}/\text{min}$ , and increased to  $700 \mu\text{m}$  by increasing the flowing speed to  $150 \mu\text{L}/\text{min}$ . The bead size linearly depended on the flowing speed of polymer solution  $v_{\text{PS}}$ . So it is quite easy to predict the bead size before the fabrication. When the 7% polystyrene solution injection speed is  $150 \mu\text{L}/\text{min}$ , 176 droplets will be generated per minute and therefore 167 beads with diameter of  $700 \mu\text{m}$  will be obtained. The diversity of the bead sizes could be controlled to be as low as 4.8% in different experiments.

The organic solvent in the droplets evaporated so the droplets were solidified into polymer beads. Because the density of the pearl pigment and polystyrene solution is  $\sim 3$  and  $1.045 \text{ g}/\text{cm}^3$ , respectively, the pearl pigment in the polystyrene solution will settle down or agglomerate on the bottom of the droplets if the solvents in the droplets are left evaporated without rotary or stirred (we call it deposition evaporation), which will result in beads endowed with nonuniform (uneven) color. When nonuniformly colored polymer beads undergo free movement and rotation in bioassay applications, they will be incorrectly decoded due to the spatial orientation of the pigment component. For example, in Figure 6A the nonuniformly colored beads are transparent from some angles. While in Figure 6C uniformly colored beads randomly distributed in a micro-well were purple from any angle. The problem can be solved by using rotary evaporation. When the rotary speed was faster than 40 rpm, uniformly colored polymer beads were gained. Figure 6 shows the nonuniformly colored beads formed by deposition evaporation and the uniformly colored beads formed by rotary evaporation. Since the color of the beads

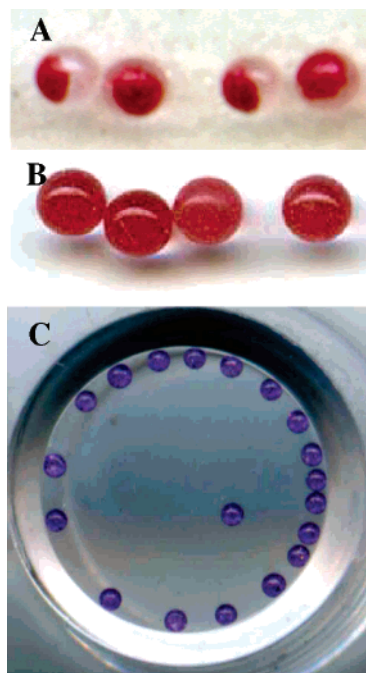


**Figure 6.** (A) Nonuniformly colored beads formed by deposition evaporation. (B) Uniformly colored beads formed by rotary evaporation. (C) Image showing uniformly colored purple beads randomly distributed in a micro-well are the same color from any angle.

comes from many pigment flakes dispersed evenly and randomly in the beads and is an average effect of light reflection from these flakes, the beads exhibit uniform color from any angle. The uniformly colored beads could be decoded irrespective of the rotation of the beads. Both the color and surface properties of the encoded beads are very stable. No obvious change was observed even if they were stored in room temperature for over 3 months or treated with high temperature up to  $80 \text{ }^\circ\text{C}$ . There is no specific demand for the storage and transport of the optical encoded beads unlike the fluorescence microspheres which usually need to be stored at  $2\text{--}8 \text{ }^\circ\text{C}$ .<sup>40</sup>

The polystyrene material differs from pearl pigment in the capability of biomolecule adsorption or binding. However, a surface with defined capacity for the immobilized biomolecules is very important in bioassay applications. For pearl pigment embedded spheres, if the pearl pigment for encoding appears on the bead surface, it will result in a heterogeneous surface. And the amount of the pearl pigment on the surface could hardly be controlled. The problem will be solved if only polystyrene is on the bead surface. Furthermore, polystyrene can strongly absorb protein molecules and is widely applied in biodetection and cell culture as the material of a microtiter plate. Hence, in order to make the bead surface uniform and robust, it is important to make sure that the bead is spherical and pearl pigment does not appear on it. It was found that the concentration of pearl pigment and its wettability have an effect on the homogeneity of the bead surface. First, the pearl pigment in the polymer solution could not be too concentrated. Figure 7A shows a bead fabricated with a polymer solution containing  $20 \text{ mg}/\text{mL}$  pearl pigment.

(40) [http://luminexcorp.custhelp.com/cgi-bin/luminexcorp.cfg/php/enduser/std\\_alp.php.sss](http://luminexcorp.custhelp.com/cgi-bin/luminexcorp.cfg/php/enduser/std_alp.php.sss) (accessed 2005).

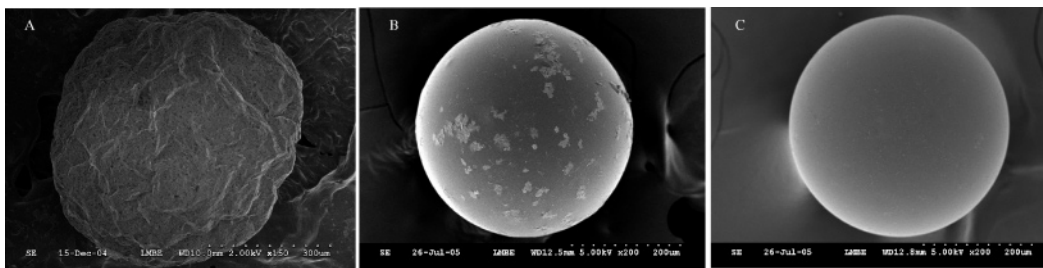


**Figure 7.** (A) Bead has high pearl pigment concentration; (B) pearl pigment is not treated with trimethylchlorosilane; (C) pearl pigment is treated with trimethylchlorosilane.

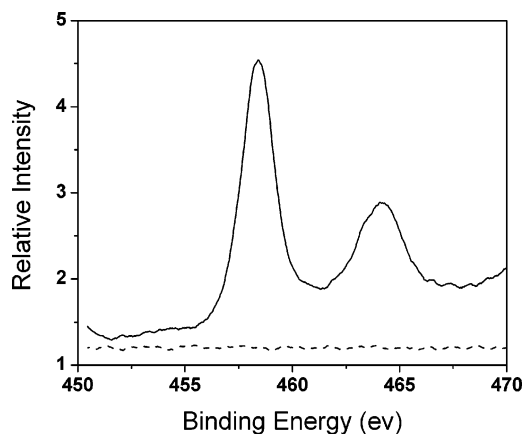


**Figure 8.** Ti 2p spectra of green pearl pigment (solid line) and polystyrene beads encoded with green pearl pigment (dashed line).

It can be observed that the bead turned out to be irregularly shaped at this concentration. Experiment showed that when the concentration of pearl pigment is lower than 1 mg/mL, spherical beads can be fabricated. Figure 6B shows the bead fabricated with the polymer solution containing 0.6 mg/mL pearl pigment. It can be observed that the bead is spherical. The other factor affecting the bead shape is the wettability of the pearl pigment. Because of the hydrophilic oxide on the surface, pearl pigment prefers to be stabilized in watery phase solution rather than the oily phase such as benzene and 1,2-dichloroethane. As a result, pearl pigment moved to the interface between the polymer solution droplet and water solution. In this situation, pearl pigment appears on the surface of the beads after solidification, which can make the surface of the bead rough and heterogeneous. It can be avoided by making the surface of pearl pigment oleophilic, which stabilizes the pearl pigment in the oily solution. The pearl pigment was mixed with 10% trimethylchlorosilane in toluene and then filtered and baked at 80 °C for 2 h before they were mixed with polystyrene solution. Figure 7C shows the bead fabricated with the pearl pigment modified by trimethylchlorosilane. It can be observed that there is no pearl pigment on the bead surface and the surfaces becomes homogeneous and relatively smooth. In addition, the surfaces of the beads were also analyzed with X-ray photoelectron spectra (XPS) (Figure 8). No peaks ascribed to Ti 2p<sub>3/2</sub> (458.5 eV) and Ti 2p<sub>1/2</sub> (464.2 eV) were observed. This indicates that the surfaces are composed of only polystyrene and the pearl dyes are embedded inside the beads.

Since our polystyrene beads were formed in the solution of PVA, which acts as a stabilizer of the oily droplets in the water solution and adheres to the surfaces of the beads, the adsorption of protein molecules will be decreased. So PVA

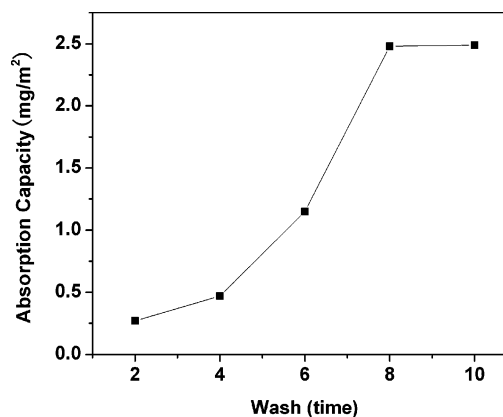


**Figure 9.** Protein adsorption capacity after a varying number of ultrasonic washings at 80 °C.

should be eliminated from the bead surface before protein immobilization. In our experiment the PVA was removed from the bead surface by repetitive ultrasonic washing. And in order to evaluate the washing effect, FITC tagged goat anti-human IgG was used to measure the protein adsorption capacity of the beads. It was found that the protein adsorption capacity increased with the washing times. And after eight washings the adsorption capacity was 2.48 mg/m<sup>2</sup> and did not increase obviously with the washing times (Figure 9). Thus, eight ultrasonic washings at 80 °C were adopted in our following experiments.

Solid-phase fluorescence immunoassay (FIA) is a convenient and rapid method to detect biomolecule binding events and is frequently used in protein microarray technique.<sup>21,41</sup> To demonstrate the reliability of our optical encoding method in multiplex immunoassay, the multicolored encoded beads were used as carriers for solid-phase FIA. Figure 9A shows the principle of our experiment. Different antigens are immobilized on polymer beads encoded with pearl pigment. After incubation with labeled antibodies that could interact with different antigens, the fluorescence on the beads encoding different binding events is measured. When there is fluorescence on the bead surface, it is indicated that the labeled antibody binding the antigen on the bead exists in the sample. We immobilized human IgG, rabbit IgG, and mouse IgG on red, yellow, and green polystyrene beads with a diameter of about 400 μm by physical adsorption. After exposure to a solution containing FITC tagged goat anti-human IgG and goat anti-rabbit IgG, the fluorescence was scanned by a laser scan confocal microscope (Figure 10B,C).

(41) Stoll, D.; Templin, M. F.; Schrenk, M.; Traub, P. C.; Vohringer, C. F.; Joos, T. O. *Front. Biosci.* **2002**, *7*, C12–C32.



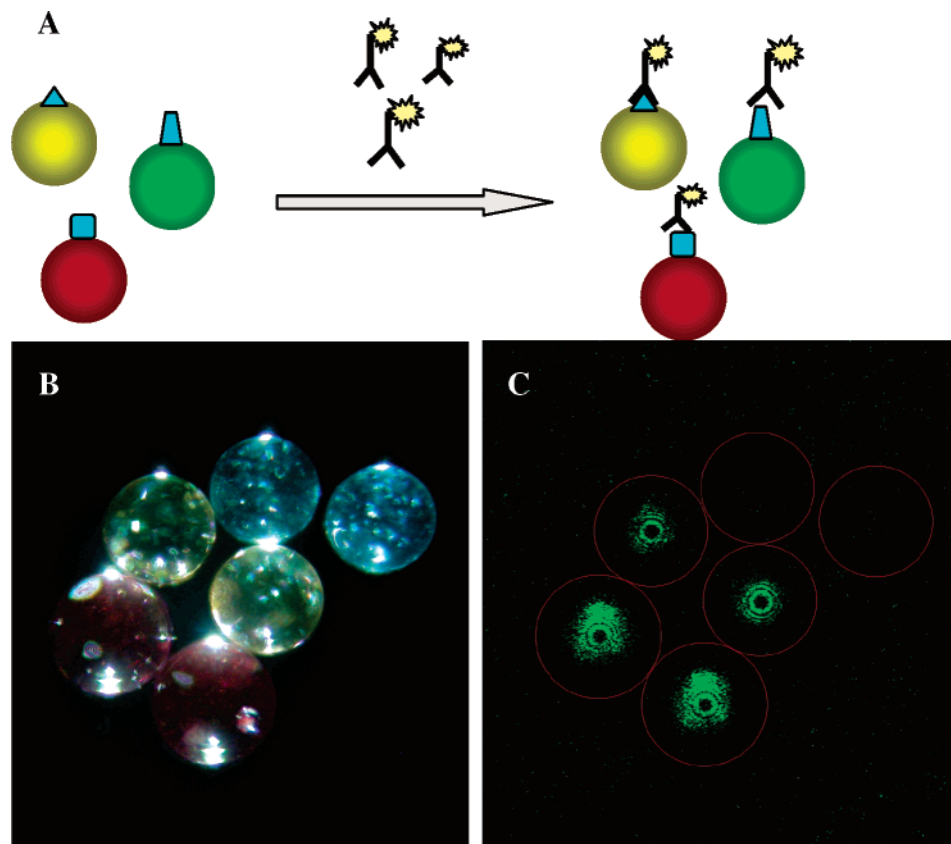


**Figure 10.** (A) Image showing the principle of multiplex immunoassay based on multicolored beads: Different antigens are immobilized on individual multicolored beads. After incubation with labeled antibodies that could interact with different antigens, beads encoding different binding events are detected. When there is a signal on a bead, the labeled antibody binding the antigen on the bead exists in the sample. (B and C) Bright field (left) and fluorescence microscope images (right) of encoded beads in a multiplexed bioassay. The beads are outlined with red circles and optical confocal slices of  $87.6\ \mu\text{m}$  in the  $z$ -direction were taken on hemispheres. Red and yellow beads coated with human IgG and rabbit IgG, respectively, show fluorescence after exposure to solution containing FITC tagged goat anti-human IgG and goat anti-rabbit IgG.

Because the beads are three-dimensional, we made optical slices of the beads with LSCM in the  $z$  direction of  $87.6\ \mu\text{m}$ . And the fluorescence image was a combination of 16 optical slices. In this experiment human IgG, rabbit IgG, and mouse IgG were encoded with red, yellow, and green polymer beads, respectively. From the two images it can be found that on yellow and red beads there are fluorescent signals while on the green beads there are no fluorescent signals. Hence, in the sample solution there was goat anti-human IgG and goat anti-rabbit IgG but no goat anti-mouse IgG. Because the codes were read under the bright field (the pictures were taken with  $10\times$  object lens) or even with eyes, optical systems with high resolution, which was employed in decoding metallic barcodes,<sup>9</sup> was not needed. And since the decoding of the carriers did not need additional exciting laser or fluorescence filter unlike that of fluorescent molecules or quantum dot encoded particles,<sup>6,8</sup> the analytical process was greatly simplified. It is expected that the encoded bead will be an alternative for a widely used microtiter plate based on the fact that Enzyme-Linked Immunosorbent Assay (ELISA) could analyze only one analyte in a sample.

## Conclusion

In conclusion, we have reported a multiplexed coding strategy based on the unique optical properties of a photonic crystal of pearl pigment. With a droplet generator apparatus we obtained uniform encoded polystyrene beads by the solvent evaporation method. The influencing factors for the encoding method were discussed and good, encoded polymer beads with homogeneous surfaces and uniform encoding colors were obtained. A simple multiplex immunoassay demonstrated that the code was stable and efficient. It is expected that the encoded bead will be an alternative for the widely used microtiter plate. We envision that the simple and cost-effective encoding strategy can be used in genomic or proteomic studies, drug screening, clinical diagnostics, and combinatorial chemical applications.

**Acknowledgment.** This work was supported by the National Natural Science Foundation of China (Grant Nos. 60228002, 20573018, 60121101) and the Ministry of Education (Grant Nos. 2004527, 20040286024).

CM060283F